Inorganic Chemistry
including bioinorganic chemistry

May 5, 2014
Volume 53, Number 9
pubs.acs.org/IC

Toward the Octupolar Cube and Giant Quadratic Hyperpolarizability

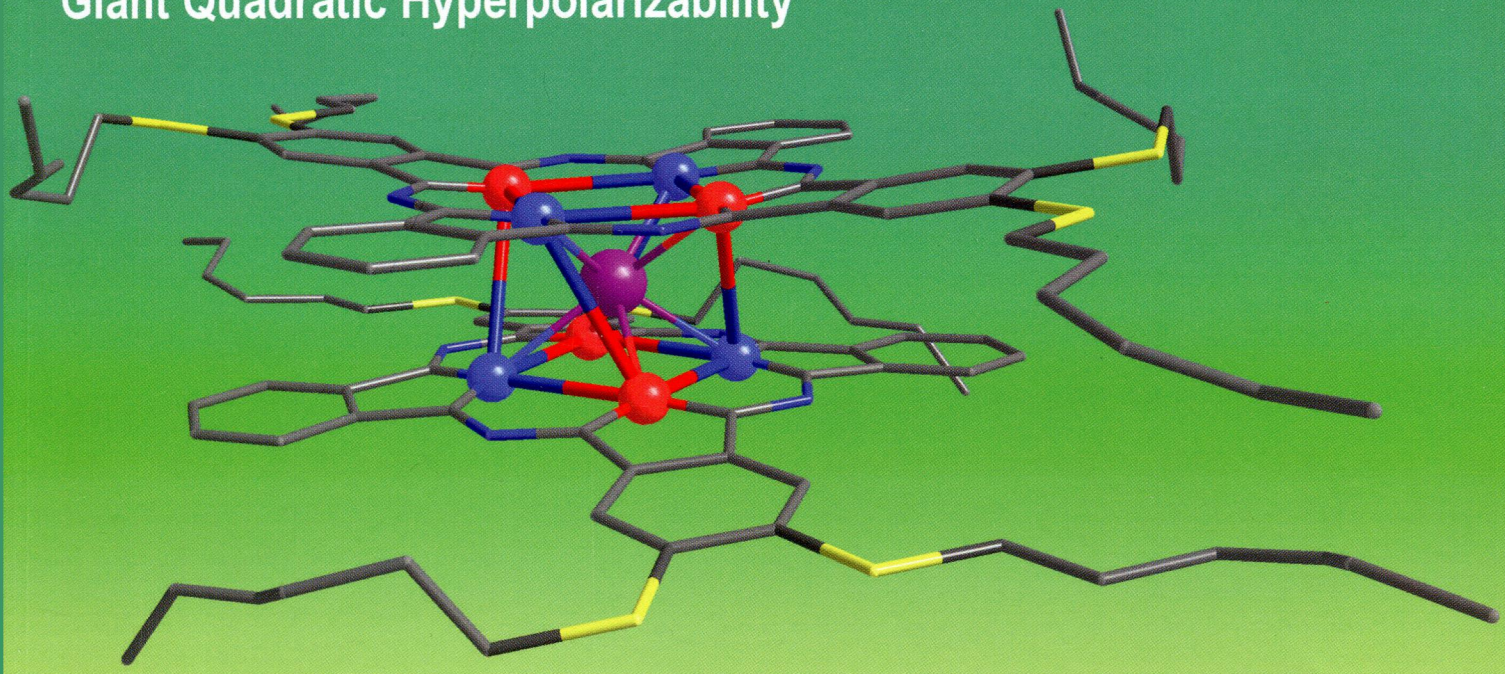

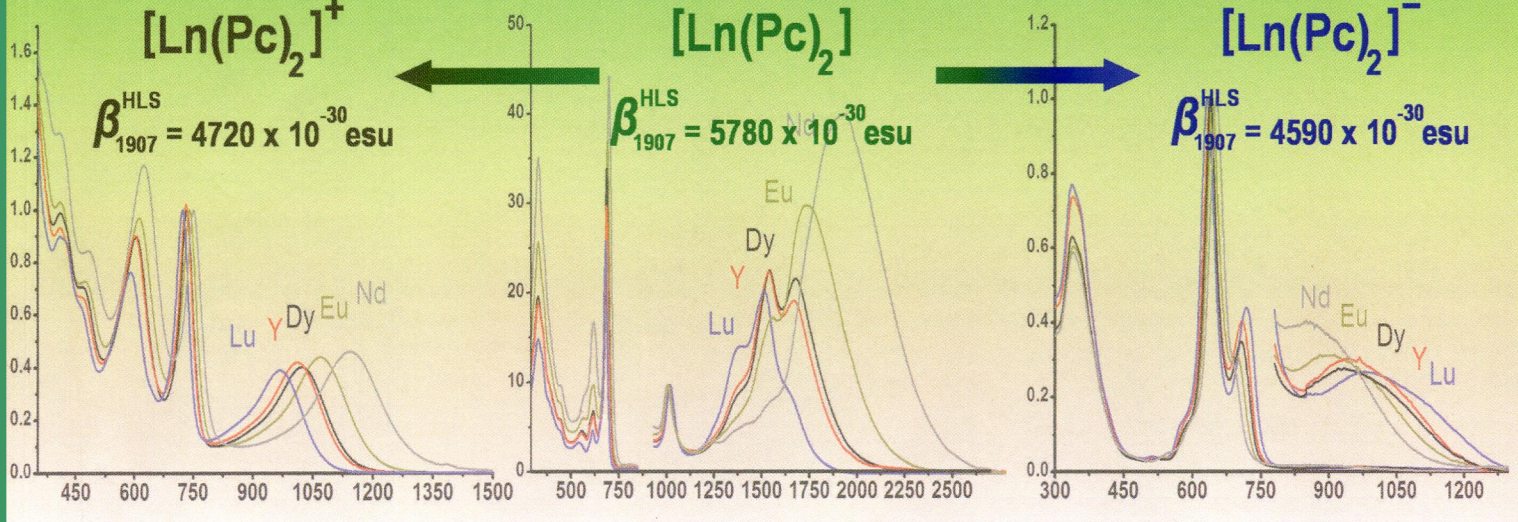

ACS Publications
Most Trusted. Most Cited. Most Read.

www.acs.org

Inorganic Chemistry

MAY 5, 2014
VOLUME 53 ISSUE 9
INOCAJ 53(9) 4269–4790 (2014)
ISSN 0020-1669

ON THE COVER: Bis(phthalocyaninato)lanthanide(III) double-decker complexes $[Ln(Pc)_2]$ of a crosswise ABAB phthalocyanine ligand were designed to closely match the structure of the octupolar cube. The highest quadratic hyperpolarizability ever reported for an octupolar molecule was measured on the neutral complexes, and the oxidized and reduced species also displayed huge values of hyperpolarizabilities. See M. M. Ayhan, A. Singh, E. Jeanneau, V. Ahsen, J. Zyss, I. Ledoux-Rak, A. G. Gürek, C. Hirel, Y. Bretonnière, and C. Andraud, p 4359.

Communications

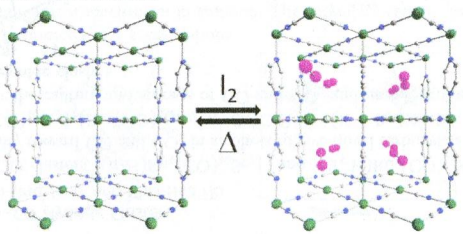

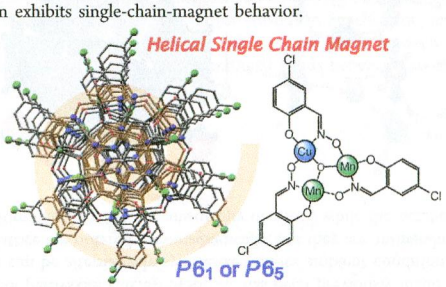

4275 S dx.doi.org/10.1021/ic500285m

Ferromagnetic Coupling in Copper(II) [2 × 2] Grid-like Complexes

Augustin M. Madalan, Xiao-Yu Cao, Guillaume Rogez, and Jean-Marie Lehn*

Two copper(II) [2 × 2] grid-like complexes with bis(hydrazone) ligands were synthesized and structurally characterized by X-ray diffraction. Investigation of the magnetic properties showed for both the occurrence of intramolecular ferromagnetic interactions.

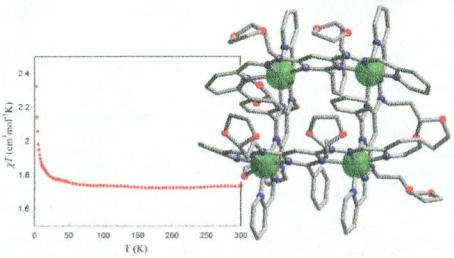

4278 S dx.doi.org/10.1021/ic500315z

A Highly Stable 3D Acentric Zinc Metal–Organic Framework Based on Two Symmetrical Flexible Ligands: High Second-Harmonic-Generation Efficiency and Tunable Photoluminescence

Jin-Shuang Guo, Gang Xu, Xiao-Ming Jiang, Ming-Jian Zhang, Bin-Wen Liu, and Guo-Cong Guo*

A 3D acentric metal–organic framework displaying large second-harmonic-generation efficiency and ultraviolet-to-visible tunable emission has been designed and prepared through a new strategy using zinc(II) and mixed symmetrical flexible ligands.

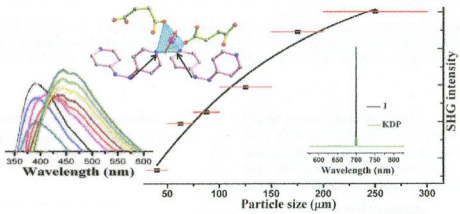

4281 (S) dx.doi.org/10.1021/ic500458m

New Routes to Synthesizing an Ordered Perovskite $CaCu_3Fe_2Sb_2O_{12}$ and Its Magnetic Structure by Neutron Powder Diffraction

Sebastian A. Larregola, Jianshi Zhou,* Jose A. Alonso, Vladimir Pomjakushin, and John B. Goodenough

Synthesis of the ordered quadruple perovskite $CaCu_3Fe_2Sb_2O_{12}$ has been previously made under high pressure. We have demonstrated that the perovskite can be alternatively synthesized under ambient condition. As determined by neutron diffraction, spins on the Fe^{3+} sublattice are ordered ferromagnetically, but they are antiparallel to spins on Cu^{2+}. The easy axis of the collinear spin ordering is dominated by the site anisotropy on Cu^{2+}, while the octahedral-site rotation has a negligible influence on it.

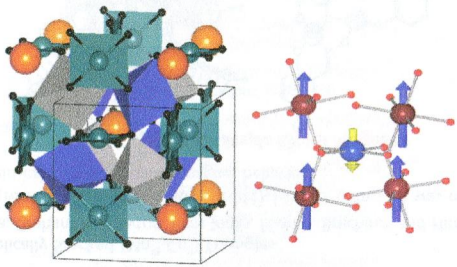

4284 (S) dx.doi.org/10.1021/ic500821z

CO and CO_2 Fixation by Se–Ru–CO Hydride Clusters

Minghuey Shieh,* Yen-Yi Chu, Li-Fing Jang, and Chia-Hua Ho

The protonic hydrido Se–Ru–CO clusters $[(\mu\text{-H})Ru_4(CO)_{10}Se_2]^-$ and $[(\mu_3\text{-H})Ru_5(CO)_{14}Se]^-$ were synthesized and demonstrated extraordinary affinity toward CO and CO_2 in alcohols to give novel carboxylate- and alkylcarbonate-bridged di-HRu_4Se_2 clusters $[\{(\mu\text{-H})Ru_4(CO)_{10}Se_2\}_2\{Ru_2(CO)_4(\mu\text{-}\eta^1\text{:}\eta^1\text{-OOCX})\}]^{3-}$ (X = R, OR; R = Me, Et). The results disclosed herein provide a new avenue for the capture and storage of CO and CO_2 and useful synthetic routes to $RCOO^-$- and $ROCOO^-$-bridged ruthenium selenide clusters.

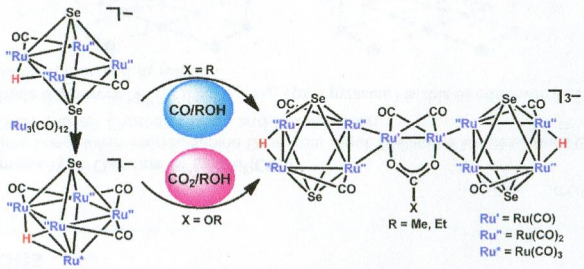

Articles

4316 S dx.doi.org/10.1021/ic500251x

$Ni_3Cl_{2.1}(OH)_{3.9}\cdot 4H_2O$, the Ni Analogue to $Mg_3Cl_2(OH)_4\cdot 4H_2O$

Sebastian Bette, Robert E. Dinnebier, and Daniela Freyer*

Surprisingly the Ni phase $Ni_3Cl_{2.1}(OH)_{3.9}\cdot 4H_2O$, characterized by thermal analysis, IR spectroscopy, scanning electron microscopy, and X-ray powder diffraction (crystal structure), is found to be isostructural to $Mg_3Cl_{2.0}(OH)_{4.0}\cdot 4H_2O$. It is the first known basic transition metal hydrate that is isostructural to a Mg-hydrate phase. All previously known basic divalent transition-metal chloride hydrates show vast differences both in the phase composition and in crystal structure constitution to basic magnesium chloride (hydrates) phases.

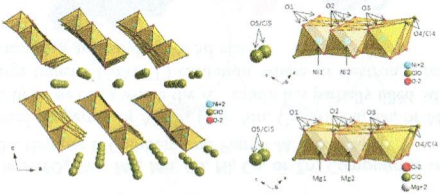

4325 S dx.doi.org/10.1021/ic403013d

Hydroxide-Bridged Cubane Complexes of Nickel(II) and Cadmium(II): Magnetic, EPR, and Unusual Dynamic Properties

Daniel L. Reger,* Andrea E. Pascui, Perry J. Pellechia, Mark D. Smith, Julia Jezierska, and Andrew Ozarowski*

Nickel(II) and cadmium(II) compounds with a hydroxide-bridged cubane core supported by a ditopic bis(pyrazolyl)methane ligand, $[M_4(\mu\text{-}OH)_4(\mu\text{-}L_m)_2(solvent)_4](ClO_4)_4$, where solvent = DMF, H_2O, acetone, were synthesized and characterized by a series of NMR, magnetic, and EPR measurements. The cadmium(II) compound shows dynamic behavior following the "Columbia Twist and Flip" rearrangement mechanism in solution. The nickel(II) centers are ferromagnetically coupled; results are supported by "broken symmetry" DFT calculations.

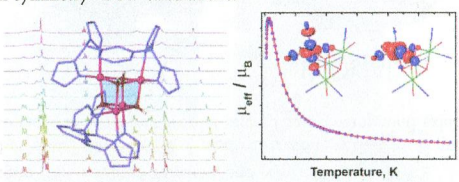

4340 S dx.doi.org/10.1021/ic403040u

Identification of the Vibrational Modes in the Far-Infrared Spectra of Ruthenium Carbonyl Clusters and the Effect of Gold Substitution

Trystan Bennett, Rohul H. Adnan, Jason F. Alvino, Vladimir Golovko,* Gunther G. Andersson,* and Gregory F. Metha*

Far-infrared spectra of the chemically synthesized, ligated, clusters $Ru_3(CO)_{12}$, $H_4Ru_4(CO)_{12}$, and $Ru_3(\mu\text{-}AuPPh_3)(\mu\text{-}Cl)(CO)_{10}$ were recorded within the region 50–650 cm^{-1} at the Australian Synchrotron, and interpreted utilizing data from DFT calculations. Vibrational frequency calculations closely predict intense peaks between 550 and 600 cm^{-1} due to metal–ligand vibrations, as well as the weaker metal core vibrational bands between 150 and 170 cm^{-1} for each cluster.

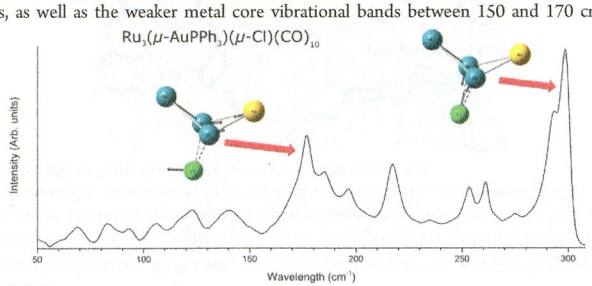

4350 S dx.doi.org/10.1021/ic4031377

Site-Specific Copper-Catalyzed Oxidation of α-Synuclein: Tightening the Link between Metal Binding and Protein Oxidative Damage in Parkinson's Disease

Marco C. Miotto, Esaú E. Rodriguez, Ariel A. Valiente-Gabioud, Valentina Torres-Monserrat, Andrés Binolfi, Liliana Quintanar, Markus Zweckstetter, Christian Griesinger, and Claudio O. Fernández*

In this work, we studied the details of Cu^{I} binding to the high-affinity interface of the protein α-synuclein by NMR spectroscopy. Our findings support a mechanism where the interaction of α-synuclein with copper ions leads to site-specific metal-catalyzed oxidation in the protein under physiologically relevant conditions.

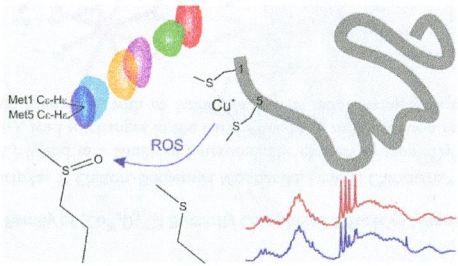

4359 S dx.doi.org/10.1021/ic4031188

ABAB Homoleptic Bis(phthalocyaninato)lanthanide(III) Complexes: Original Octupolar Design Leading to Giant Quadratic Hyperpolarizability

Mehmet Menaf Ayhan, Anu Singh, Erwann Jeanneau, Vefa Ahsen, Joseph Zyss, Isabelle Ledoux-Rak, Ayşe Gül Gürek, Catherine Hirel,* Yann Bretonnière,* and Chantal Andraud

Octupolar phthalocyanine–lanthanide double-decker complexes were specifically designed to closely match the symmetry of the octupolar cube. The size of the lanthanide (III) central ion strongly influences the optical properties. The first oxidized and reduced states of the complexes, while keeping a similar octupolar structure, display considerably changed optical properties. Exceptionally large dynamic molecular first hyperpolarizabilities were found that showed a strong dependence on the number of 4f electrons.

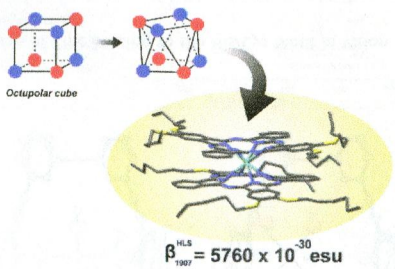

4371 S dx.doi.org/10.1021/ic403156h

Copper(II) and Gallium(III) Complexes of *trans*-Bis(2-hydroxybenzyl) Cyclen Derivatives: Absence of a Cross-Bridge Proves Surprisingly More Favorable

Catarina V. Esteves, Joana Madureira, Luís M. P. Lima, Pedro Mateus, Isabel Bento, and Rita Delgado*

Two bis(phenolate) cyclen derivatives were synthesized, one of them containing an ethylene cross-bridge. Both compounds were studied in solution and in solid state regarding their complexation ability toward Cu^{2+} and Ga^{3+} cations. Surprisingly, the compound without the cross-bridge was revealed to be the best chelator for the coordination of Cu^{2+} and also Ga^{3+}, from the thermodynamic stability as well as from the kinetic inertness of the complexes.

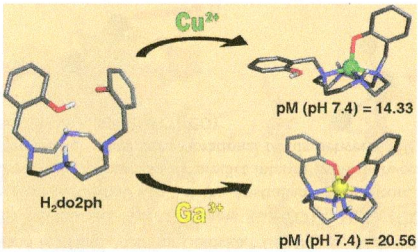

4387 S dx.doi.org/10.1021/ic403168v

Crystal Growth, Structural, Electrical, and Magnetic Properties of Mixed-Valent Compounds $YbOs_2Al_{10}$ and $LuOs_2Al_{10}$

Xu Zhang, Wei Yi, Kai Feng, Desheng Wu, Yifeng Yang, Ping Zheng, Jiyong Yao, Yoshitaka Matsushita, Akira Sato, Hongwei Jiang, Hai Wang,* Youguo Shi,* Kazunari Yamaura, and Nanlin Wang

5d compounds $YbOs_2Al_{10}$ and $LuOs_2Al_{10}$ crystallize in a cagelike structure with a space group *Cmcm*. The crystals exhibit irregular morphology with flat surfaces and millimeter-order sizes. The Yb compound exhibits mixed-valent behavior over temperatures up to 900 K.

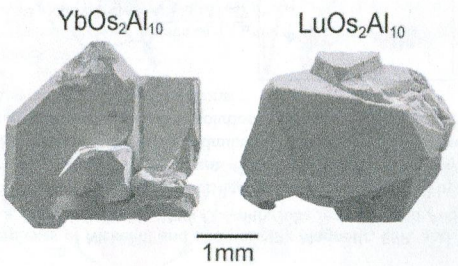

4394 S dx.doi.org/10.1021/ic4031798

Metal-to-Metal Charge Transfer in AWO_4 (A = Mg, Mn, Co, Ni, Cu, or Zn) Compounds with the Wolframite Structure

Swagata Dey, Rebecca A. Ricciardo, Heather L. Cuthbert, and Patrick M. Woodward*

The electronic structures and optical properties of AWO_4 (A = Mn, Co, Ni, Cu, Zn, or Mg) tungstates with the wolframite structure have been characterized. In those cases where the A^{2+} cation has partially filled 3d orbitals, the lowest energy optical excitation is a metal-to-metal charge transfer (MMCT) excitation, where an electron is transferred from the occupied 3d orbitals of the A^{2+} ion to the unoccupied antibonding W 5d states.

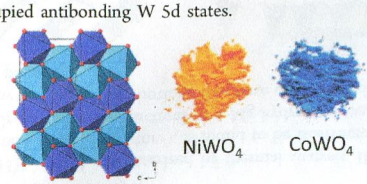

4400 S dx.doi.org/10.1021/ic500065s

K–H_3C and K–Sn Interactions in Potassium Trimethylstannyl Complexes: A Structural, Mechanochemical, and NMR Study
Christian Kleeberg,* Jörg Grunenberg,* and Xiulan Xie*

K–H_3C–$Sn(CH_3)_2$ and K–$Sn(CH_3)_3$ interactions are, in the solid state, structurally important for a series of potassium trimethylstannyl complexes. For the unsymmetrical anion $[Me_2SnCH_3–K–SnMe_3]^-$ both interactions are, according to computational data, of comparable strength, and the unsymmetrical coordination mode is thermodynamically favored over both symmetrical isomers. A concomitant NMR study revealed the existence of multiple species in THF and PhMe.

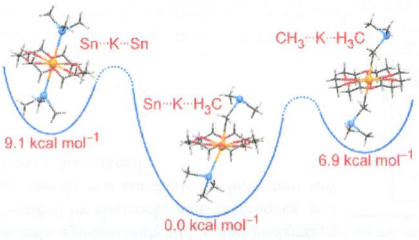

4411 S dx.doi.org/10.1021/ic5000765

4,5-Dicyano-3,6-diethylbenzo-1,2-diselenete, a Highly Stable 1,2-Diselenete: Its Preparation, Structural Characterization, Calculated Molecular Orbitals, and Complexation with Tetrakis(triphenylphosphine)palladium
Takeshi Kimura,* Tsukasa Nakahodo, Hisashi Fujihara, and Eiichi Suzuki

The first isolable benzo-1,2-diselenete, 3,6-diethyl-4,5-dicyanobenzo-1,2-diselenete (**4**), was prepared by the reaction of 4,5-(*o*-xylylenediseleno)-3,6-diethylphthalonitrile (**3**) with aluminum chloride in toluene. X-ray crystallographic analysis demonstrated that **4** contains a trapezoidal diselenide ring rather than a benzo-1,2-diselenone structure. The reaction of **4** with tetrakis(triphenylphosphine)palladium in benzene was found to produce a dinuclear palladium complex (**8**).

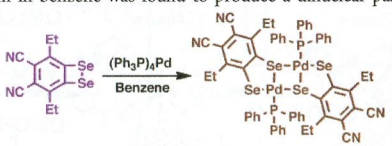

4418 S dx.doi.org/10.1021/ic5000793

The Synthesis of a Corrole Analogue of Aquacobalamin (Vitamin B_{12a}) and Its Ligand Substitution Reactions
Caitlin F. Zipp, Joseph P. Michael, Manuel A. Fernandes, Sadhna Mathura, Christopher B. Perry, Isabelle Navizet, Penny P. Govender, and Helder M. Marques*

Equilibrium constants for the substitution of H_2O by a variety of neutral and anionic ligands in a corrole analogue of aquacobalamin (vitamin B_{12a}) and in aquacobalamin itself are reported, and the effect of changing the equatorial macrocycle on the reactions of Co(III) complexes is assessed.

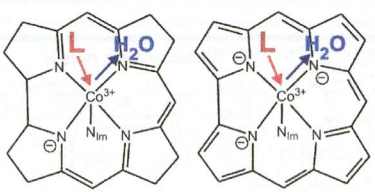

4430 dx.doi.org/10.1021/ic500089b

Photochemical Dihydrogen Production Using an Analogue of the Active Site of [NiFe] Hydrogenase

Peter A. Summers, Joe Dawson, Fabio Ghiotto, Magnus W. D. Hanson-Heine, Khuong Q. Vuong, E. Stephen Davies, Xue-Z. Sun, Nicholas A. Besley, Jonathan McMaster,* Michael W. George,* and Martin Schröder*

Light-driven electron transfer to $[NiFe_2]$ ($[Ni(L)Fe_2(CO)_6]$, $L^{2-} = (CH_3C_6H_3S_2)_2(CH_2)_3$) using $[ReCl(CO)_3(bpy)]$ as a photosensitizer and NEt_3 as a sacrificial electron donor forms the basis of photocatalytic H_2 production using a low molecular weight [NiFe] hydrogenase mimic.

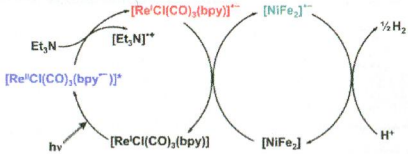

4440 dx.doi.org/10.1021/ic500094b

Large-Scale Synthesis of Well-Dispersed Copper Nanowires in an Electric Pressure Cooker and Their Application in Transparent and Conductive Networks

Shenjie Li, Yanyan Chen, Lijian Huang, and Daocheng Pan*

We present a novel large-scale synthetic method for well-separated copper nanowires (CuNWs) in a commercial electric pressure cooker under mild reaction conditions. CuNWs (~2.1 g) can be prepared in a batch with direct materials cost of $4.20/g. Well-dispersed polyvinylpyrrolidone-capped CuNWs were obtained via a ligand-exchange method. The transparent and conductive CuNW networks with excellent electrical conductivity and high optical transmittance (30 Ω/□ at 86% transmittance) were fabricated by a spin-coating process.

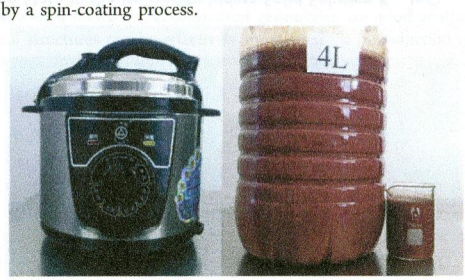

4445 dx.doi.org/10.1021/ic500100e

Selective Synthesis of Cu_2SnSe_3 and Cu_2SnSe_4 Nanocrystals

Zhen-Hua Ge, James R. Salvador, and George S. Nolas*

Cu_2SnSe_3 and Cu_2SnSe_4 nanocrystals were selectively synthesized employing a one-step solvothermal method by using different Cu and Sn sources. When CuCl was used as the Cu source Cu_2SnSe_3 nanocrystals (25 nm) were obtained. When $CuCl_2$ was used as the Cu source Cu_2SnSe_4 nanocrystals (45 nm) were obtained.

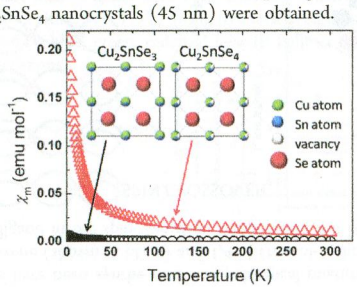

4450 dx.doi.org/10.1021/ic500102c

Isolation of Iron(II) Aqua and Hydroxyl Complexes Featuring a Tripodal H-bond Donor and Acceptor Ligand

Ellen M. Matson, Jeffrey A. Bertke, and Alison R. Fout*

A tripodal ligand platform, tris(5-cycloiminopyrrol-2-ylmethyl)amine ($H_3[N(pi^{Cy})_3]$) is reported. The ability of the ligand to tautomerize to the amino azafulvene $H_3[N(afa^{Cy})_3]$ upon substrate addition is evident in the isolation of a series of iron(II) complexes. The combined data for the iron complexes establishes that each arm of the tripodal ligand can tautomerize independently, depending on electronic needs of the iron center and substrate coordination.

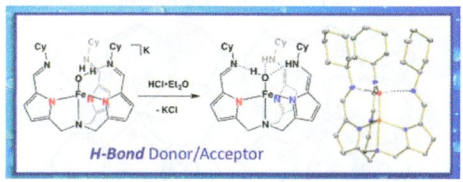

4459 dx.doi.org/10.1021/ic5001123

Iron Complexes Derived from {nacnac-$(CH_2py)_2$}$^-$ and {nacnac-$(CH_2py)(CHpy)$}^{n} Ligands: Stabilization of Iron(II) via Redox Noninnocence

Valerie A. Williams, Peter T. Wolczanski,* Jörg Sutter, Karsten Meyer, Emil B. Lobkovsky, and Thomas R. Cundari

Nanac-based tetradentate chelates, {nacnac-$(CH_2py)_2$}$^-$ ({nn$(PM)_2$}$^-$) and {nacnac-$(CH_2py)(CHpy)$}^{n} ({nn(PM)(PI)}^{n}), have been applied to iron, and the latter exhibits redox noninnocent behavior (n = 2−) in {nn(PM)(PI)}FeLL′ [2-L,L′; L,L′ = $(PMe_3)_2$, $(PMe_2Ph)_2$, $PMe_3(CO)$] and {nn(PM)(PI)}FeL (3-L; L = CO, PMe_3, $PMePh_2$, PPh_3).

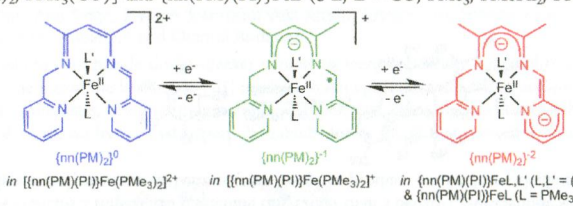

4475 dx.doi.org/10.1021/ic500122b

Unexpected NO Transfer Reaction between *trans*-$[Ru^{II}(NO^+)(NH_3)_4(L)]^{3+}$ and Fe(III) Species: Observation of a Hetero-bimetallic NO-Bridged Intermediate

Gustavo Metzker, Pietro P. Lopes, Augusto C. H. da Silva, Sebastiao C. da Silva, and Douglas W. Franco*

The reaction of ruthenium tetraamine nitrosyl complexes with Fe(III) species (FeTPPS, metMb, and Hb) leads to the NO transfer between the two metal centers by formation of a heterobimetallic species, with NO as the bridging ligand. The binuclear species was identified by electrochemical techniques, and its structure optimized by DFT. Also, specific rate constants for formation and dissociation of the binuclear species were determined.

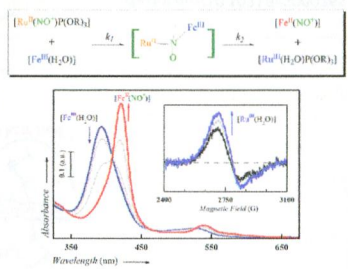

4482 dx.doi.org/10.1021/ic500141v

A Mixed-Ligand Approach for Spin-Crossover Modulation in a Linear Fe^{II} Coordination Polymer

Néstor Calvo Galve, Eugenio Coronado, Mónica Giménez-Marqués, and Guillermo Mínguez Espallargas*

A family of Fe^{II} coordination polymers have been synthesized using chemical mixtures of two different but closely related ligands, 1,4-bis(tetrazol-1-ylmethyl)benzene (shown in black) and 1,4-bis(triazol-1-ylmethyl)benzene (shown in red), and the effect of a gradual substitution of the ligand in the spin transition temperature has been investigated.

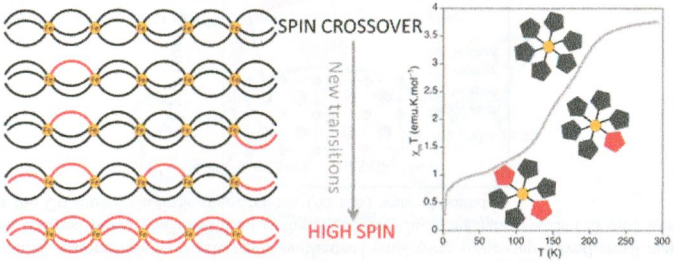

4491 dx.doi.org/10.1021/ic500151j

High-Coordinate Gold(I) Complexes with Dithiocarboxylate Ligands

Christoph Kaub, Timo Augenstein, Thomas O. Bauer, Elisa Rothe, Lars Esmezjan, Volker Schünemann, and Peter W. Roesky*

Ferrocene dithiocarboxylate has been introduced into the chemistry of gold(I) and copper(I). The ligand coordinates either in a monodentate, a chelating, or in a metal bridging mode. Monomeric, dimeric, and polymeric structures were obtained.

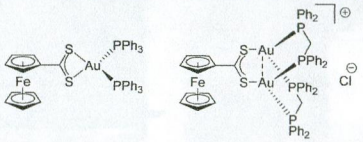

4500 dx.doi.org/10.1021/ic5001667

Control of the Iridium Oxidation State in the Hollandite Iridate Solid Solution $K_{1-x}Ir_4O_8$

Artem Talanov, W. Adam Phelan, Zachary A. Kelly, Maxime A. Siegler, and Tyrel M. McQueen*

Synthesis and properties of $K_{1-x}Ir_4O_8$ ($0 \leq x \leq 0.7$) are reported. The structure of KIr_4O_8 was solved using X-ray diffraction. A large anisotropic displacement parameter is found for potassium. Density functional theory calculations show that this anisotropy is due to a competition between size and bond valence. KIr_4O_8 has a significant electronic contribution to the specific heat. A magnetic-field-dependent upturn is observed in the specific heat below 3 K. Resistivity and magnetization show that both end-members are metallic.

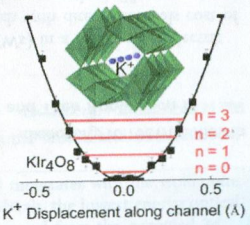

4508 dx.doi.org/10.1021/ic500180k

Interplay between Local Anisotropies in Binuclear Complexes

Renaud Ruamps, Rémi Maurice, Coen de Graaf, and Nathalie Guihéry*

The role of local distortions on the molecular magnetic anisotropies of model binuclear Ni(II) complexes is assessed with wave function based methods. The anisotropy parameters of the multispin and giant-spin model Hamiltonians are unambiguously extracted with the effective Hamiltonian theory. It is shown that the combination of some local distortions can lead to constructive or destructive interactions between the local anisotropies, which can be used to tune the magnetic anisotropy in polynuclear complexes.

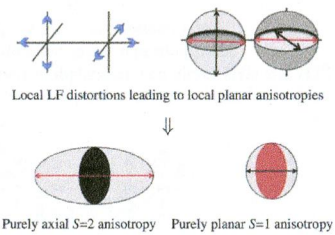

4517 dx.doi.org/10.1021/ic5002094

Nonlinear-Optical Properties of α-Diiminedithiolatonickel(II) Complexes Enhanced by Electron-Withdrawing Carboxyl Groups

Luca Pilia,* Maddalena Pizzotti, Francesca Tessore, and Neil Robertson*

Three α-diiminedithiolatonickel(II) complexes bearing electron-withdrawing carboxyl groups and showing remarkably high values of the second-order nonlinear optical properties have been prepared and characterized. The role of the carboxyl groups in enhancing β_0 has been highlighted by experimental and computational methods.

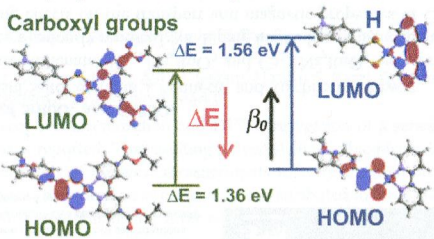

4527 dx.doi.org/10.1021/ic500218q

Light-Driven Hydrogen Evolution by BODIPY-Sensitized Cobaloxime Catalysts

Juergen Bartelmess, Aaron J. Francis, Karim A. El Roz, Felix N. Castellano, Walter W. Weare,* and Roger D. Sommer

Four hydrogen evolving cobaloxime complexes, sensitized by different structurally modified BODIPYs, were prepared and characterized. These photocatalysts generate hydrogen (turnover number (TON) of up to 31), and the influence of structural modifications on catalyst properties is probed. It is found that efficient formation of triplet states is decisive for successful proton reduction atalysis. We illustrate the importance of the interplay between catalyst stability and electron transfer efficiency for optimizing photocatalyst turnover frequency and turnover in this system.

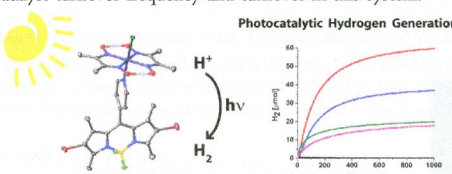

4535 Ⓢ dx.doi.org/10.1021/ic500222y

Synthesis, Structure, and Magnetic Properties of $(Tb_{1-x}Mn_y)MnO_{3-\delta}$

Hao Zhang, Roxana Flacau, Junliang Sun, Guobao Li,* Fuhui Liao, and Jianhua Lin*

Two samples $(Tb_{1-x}Mn_y)MnO_3$ ($x = 0.089$, $y = 0.063$ for W1, and $x = 0.122$, $y = 0.102$ for W2) have been synthesized by solid-state reactions with W1 showing sinusoidal antiferromagnetic orders and W2 showing both sinusoidal antiferromagnetic and canted commensurate antiferromagnetic orders.

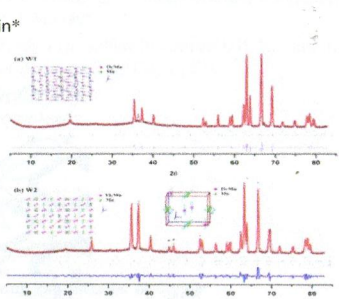

4541 Ⓢ dx.doi.org/10.1021/ic500224m

Turn Helical Motifs from Pair to Single Entangled Double Helixes in a Cobalt–Vanadate System via Introduction of a V-Shaped Ligand

Shaobin Li, Wenlong Sun, Kun Wang, Huiyuan Ma,* Haijun Pang,* Heng Liu, and Jianxin Zhang

Two novel helical compounds based on polyoxovanadates have been synthesized. Compound **1** shows an unprecedented helical disposition type, namely, possessing a pair of entangled double helixes in a 3D inorganic framework. Compound **2** has a single of entangled double helixes in a 3D inorganic–organic network. The isolation of these two compounds demonstrates that the vanadium oxide polyhedra with multiform coordination geometries are good synthons for the synthesis of novel helical compounds and the helical structures can be effectively modulated via introduction of a proper ligand.

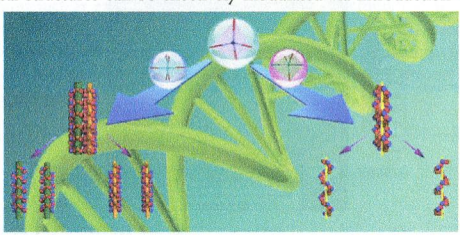

4548 Ⓢ dx.doi.org/10.1021/ic5002368

***In Vitro* Multiwavelength PDT with ^{3}IL States: Teaching Old Molecules New Tricks**

Huimin Yin, Mat Stephenson, Jordan Gibson, Eric Sampson, Ge Shi, Tariq Sainuddin, Susan Monro, and Sherri A. McFarland*

Low-lying, long-lived ^{3}IL excited states can be exploited for multiwavelength photodynamic therapy (PDT) in Ru(II) complexes that are traditionally recognized as blue-green absorbers. This work demonstrates unequivocally that compounds once thought to have less utility as photosensitizers for PDT, owing to a lack of significant absorption in the phototherapeutic window (600–850 nm), can be triggered by blue, green, red, and near-IR light in order to act as potent light-sensitive cytotoxic agents for photodynamic applications.

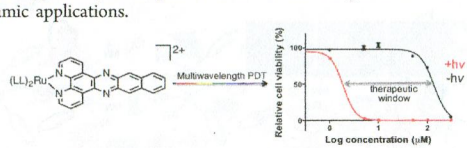

4560 Ⓢ dx.doi.org/10.1021/ic5001649

Modulating the Sensor Response to Halide Using NBD-Based Azamacrocycles

Stefano Amatori, Gianluca Ambrosi, Elisa Borgogelli, Mirco Fanelli, Mauro Formica, Vieri Fusi,* Luca Giorgi, Eleonora Macedi, Mauro Micheloni, Paola Paoli, Patrizia Rossi, and Aurora Tassoni

Ligand **L** is a fluorescent ditopic ligand containing two cyclen tetraazamacrocycle moieties connected to a phenol unit and bearing two NBD fluorophores. The Zn(II) dinuclear complex of this ligand acts as a metallo receptor for chloride anions. The signal transduction consists of an increase in its emission intensity upon chloride addition in an acetonitrile/water 95:5 (v/v) solution.

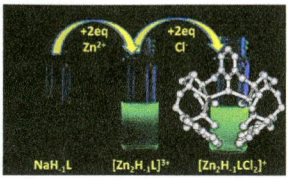

4570 Ⓢ dx.doi.org/10.1021/ic500252c

One-Step Bulk Synthesis of Stable, Near Unit-Cell Sized Oxide Nanoparticles and Nanoparticle Blends Using KO_2

Thomas E. Sutto*

This novel synthetic technique produces oxide and hydroxide nanoparticles in one simple step from salt solutions. Nanoparticles generated are typically less than 4 nm wide.

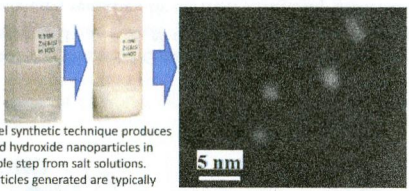

This novel synthetic technique produces oxide and hydroxide nanoparticles in one simple step from salt solutions. Nanoparticles generated are typically below 4 nm.

4579 dx.doi.org/10.1021/ic500265t

High-Concentration Na Doping of $SrRuO_3$ and $CaRuO_3$

Hayato Seki, Ryuta Yamada, Takashi Saito, Brendan J. Kennedy, and Yuichi Shimakawa*

The Na-doped perovskite-structure ruthenates $Sr_{1-x}Na_xRuO_3$ and $Ca_{1-y}Na_yRuO_3$ were prepared by high-pressure synthesis, which enables us to go beyond the previously reported Na doping limits. Ferromagnetic interaction in the Na-doped $SrRuO_3$ was suppressed, but the Na-doping effects on the transport and magnetic properties of $CaRuO_3$ were insignificant.

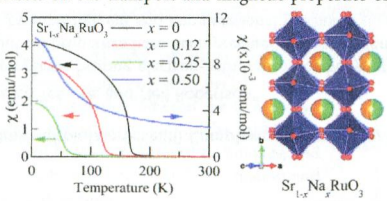

4585 dx.doi.org/10.1021/ic5002682

Silylamide Complexes of Chromium(II), Manganese(II), and Cobalt(II) Bearing the Ligands $N(SiHMe_2)_2$ and $N(SiPhMe_2)_2$

Sonja N. König, Christoph Schädle, Cäcilia Maichle-Mössmer, and Reiner Anwander*

Salt metathesis and transamination protocols give ready access to bis(dimethylsilyl)amide and bis(dimethylphenylsilyl)amide complexes of the divalent transition metals chromium, manganese, and cobalt. Depending on the metal size and the presence of donor solvent, secondary M---π(arene) interactions cause distinct coordination environments.

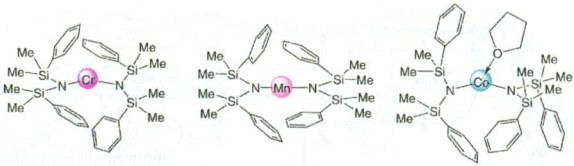

4598 dx.doi.org/10.1021/ic500284q

Uncovering the Role of Intra- and Intermolecular Motion in Frustrated Lewis Acid/Base Chemistry: *Ab Initio* Molecular Dynamics Study of CO_2 Binding by Phosphorus/Boron Frustrated Lewis Pair [tBu$_3$P/B(C$_6$F$_5$)$_3$]

Maoping Pu and Timofei Privalov*

Ab initio molecular dynamics (AIMD) study of the binding of CO_2 by a Lewis acid and a Lewis base, $B(C_6F_5)_3$ and $P(t\text{Bu})_3$, at 300 K in gas phase shows that roaming applies to complex systems and advances the concept of the "dynamical frustration" of the chemical step. The main body of results is based on reasonably large ensemble of AIMD trajectories, elucidating both the binding scenario and the return to the reactants region.

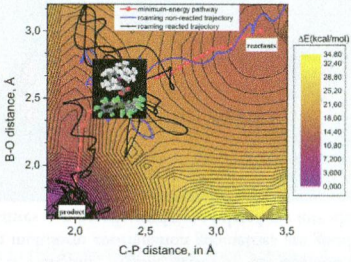

4610 dx.doi.org/10.1021/ic500288w

Conformation-Controlled Sorption Properties and Breathing of the Aliphatic Al-MOF [Al(OH)(CDC)]

Felicitas Niekiel, Jeroen Lannoeye, Helge Reinsch, Alexis S. Munn, Andreas Heerwig, Ivo Zizak, Stefan Kaskel, Richard I. Walton, Dirk de Vos, Philip Llewellyn, Alexandra Lieb, Guillaume Maurin,* and Norbert Stock*

The sorption properties of the Al-MOF CAU-13 were studied in detail. The adsorption of water and CO_2 leads to small structural changes. However, when CAU-13 is exposed to xylene, a drastic change in the crystal structure is observed. In the evacuated form, CAU-13 contains *trans*-cyclohexanedicarboxylate linkers in the e,e and a,a conformations. After the adsorption of xylene, all of the linker molecules exhibit the e,e conformation, leading to a unit cell increase of ~25%.

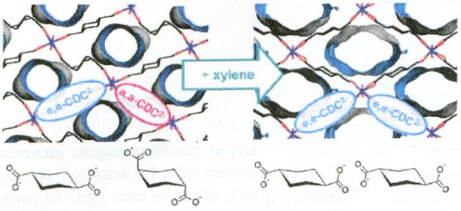

4621 S dx.doi.org/10.1021/ic500305n

Two Types of Heterometallic One-Dimensional Alignment Composed of Acetamidate-Bridged Dirhodium and Pivalamidate-Bridged Diplatinum Complexes

Kazuhiro Uemura,* Toru Kanbara, and Masahiro Ebihara

Two kinds of one-dimensional (1D) chain complexes composed of $[Rh_2(acam)_4]$ (acam = acetamidate) and $[Pt_2(piam)_2(NH_3)_4]$ (piam = pivalamidate) are shown. These compounds have different metal repeating units, $-\{Rh-Rh-Pt-Pt-Pt-Pt\}_n-$ and $-\{Rh-Rh-Pt-Pt\}_n-$, caused by different isomers of diplatinum complexes (HH and HT) and their different hydrogen bonding modes. Interestingly, expected HOMOs in these compounds are δ^* orbitals in rhodium parts, indicating that the electronic structure can be modulated by ligand tuning.

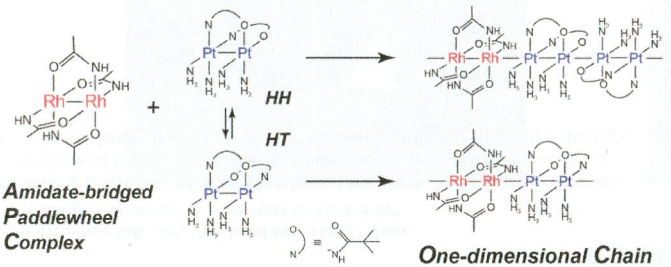

4629 S dx.doi.org/10.1021/ic500321w

Synthesis and Characterization of Silver(I) Pyrazolylmethylpyridine Complexes and Their Implementation as Metallic Silver Thin Film Precursors

Irene Bassanetti, Christina P. Twist, Myung-Gil Kim, Afif M. Seyam, Hassan S. Bazzi, Q. Jane Wang, Yip-Wah Chung, Luciano Marchió,* Massimiliano Delferro,* and Tobin J. Marks*

Synthesis, structural, and spectroscopic characterization and DFT investigation of a series of light- and air-stable silver(I) pyrazolylmethylpyridine complexes is reported. The resulting polycrystalline cubic-phase Ag films contain negligible amounts of extraneous contamination. The results of the wear measurements indicate a significant reduction in wear (~ 88%) at optimized Ag complex concentrations. Enhanced wear performance is attributed to facile shearing of Ag metal deposited in the contact region, which results from thermolysis of the silver complex.

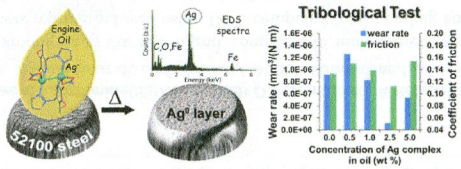

4639 dx.doi.org/10.1021/ic5003176

Sequence-Specific Cu(II)-Dependent Peptide Bond Hydrolysis: Similarities and Differences with the Ni(II)-Dependent Reaction

Agnieszka Belczyk-Ciesielska, Izabela A. Zawisza, Mariusz Mital, Arkadiusz Bonna, and Wojciech Bal*

Cu(II) ions are able to hydrolyze peptides of a general sequence R_N-(Ser/Thr)-Xaa-His-Zaa-R_C according to the same molecular mechanism as for Ni(II) ions. Their maximum reactivity at high pH is 40−300 times lower that for Ni(II) ions, but the greater ability of Cu(II) to form 4N complexes results in similar hydrolysis rates at neutral pH, providing it with biological relevance.

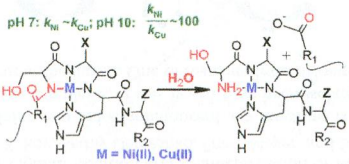

4647 S dx.doi.org/10.1021/ic500333p

Modeling Biological Copper Clusters: Synthesis of a Tricopper Complex, and Its Chloride- and Sulfide-Bridged Congeners

Gianna N. Di Francesco, Aleth Gaillard, Ion Ghiviriga, Khalil A. Abboud, and Leslie J. Murray*

Reaction of a tricopper(I) tris(β-diketiminate) cyclophane complex with sulfur affords a (μ_3-sulfido)tricopper(I/II/II) cluster, $Cu_3(\mu_3\text{-}S)\mathbf{L}$, which can be chemically reduced to the corresponding valence-delocalized species $[Cu_3(\mu_3\text{-}S)\mathbf{L}]^-$.

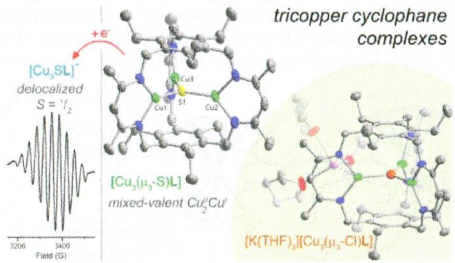

4655 S dx.doi.org/10.1021/ic500348k

Oligonuclear Fe Complexes (Fe, Fe_4, Fe_6, Fe_9) Derived from Tritopic Pyridine Bis-Hydrazone Ligands—Structural, Magnetic, and Mössbauer Studies

Muhammad U. Anwar, Louise N. Dawe, Stewart R. Parsons, Santokh S. Tandon, Laurence K. Thompson,* Subrata K. Dey, Valeriu Mereacre, William M. Reiff, and Scott D. Bunge

Tritopic pyridine bis-hydrazone ligands produce polynuclear complexes with Fe(II) and Fe(III) salts with varying nuclearity and metal ion oxidation states. Mononuclear, tetranuclear, hexanuclear, and nonanuclear examples are discussed using structural, magnetic, and Mössbauer data. In one case, although X-ray data suggest a [3 × 3] Fe_9 grid (space group $P4_2/n$), careful examination of the structure, in conjunction with magnetic and Mössbauer data, indicates an unusual situation where the corner and center sites are present at unit occupancy, whereas side site occupancy is ~0.6.

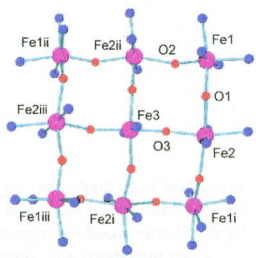

4669 S dx.doi.org/10.1021/ic500340x

Single-Crystal Growth and Size Control of Three Novel Polar Intermetallics: $Eu_{2.94(2)}Ca_{6.06}In_8Ge_8$, $Eu_{3.13(2)}Ca_{5.87}In_8Ge_8$, and $Sr_{3.23(3)}Ca_{5.77}In_8Ge_8$ with Crystal Structure, Chemical Bonding, and Magnetism Studies

Hyein Woo, Gnu Nam, Eunyoung Jang, Jin Kim, Yunho Lee, Kyunghan Ahn, and Tae-Soo You*

Three new polar intermetallic compounds—$Eu_{2.94(2)}Ca_{6.06}In_8Ge_8$, $Eu_{3.13(2)}Ca_{5.87}In_8Ge_8$, and $Sr_{3.23(3)}Ca_{5.77}In_8Ge_8$—with a novel isotypic structure type have been synthesized via a reactive indium metal-flux method. The thicknesses of bar/needle-shaped single-crystals of the Eu compounds were controlled in the micrometer scale by adjusting some reaction conditions. Magnetic susceptibility measurements proved the AFM ordering of Eu atoms below 4 K with a reduced effective magnetic moment of 7.12 μ_B/Eu for $Eu_{3.13(2)}Ca_{5.87}In_8Ge_8$.

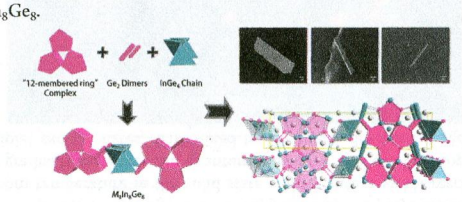

4678 dx.doi.org/10.1021/ic500355f

Introducing a New Azoaromatic Pincer Ligand. Isolation and Characterization of Redox Events in Its Ferrous Complexes
Pradip Ghosh, Subhas Samanta, Suman K. Roy, Serhiy Demeshko, Franc Meyer, and Sreebrata Goswami*

A new pincer-type neutral ligand containing two redox-noninnocent azo functions is introduced and shown to serve as a multielectron redox reservoir. Two ferrous complexes of this ligand have been isolated and thoroughly characterized, and redox processes are shown to largely occur at the ligand. One of the complexes belongs to a rare class of stable and uncoupled azo-anion radical systems.

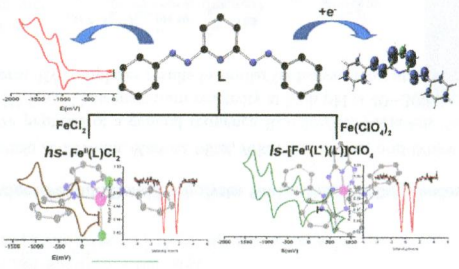

4687 dx.doi.org/10.1021/ic500361b

Selectivity of Azine Ligands Toward Lanthanide(III)/Actinide(III) Differentiation: A Relativistic DFT Based Rationalization
Abdellah Zaiter, Boudersa Amine, Yamina Bouzidi, Lotfi Belkhiri,* Abdou Boucekkine,* and Michel Ephritikhine

Higher selectivity of polyazines, among them the BPP ligand, compared to monoazines, especially for the Eu^{III}/Am^{III} pair operating in spent nuclear fuel, was reproduced well using DFT computed total bonding energy as criterion.

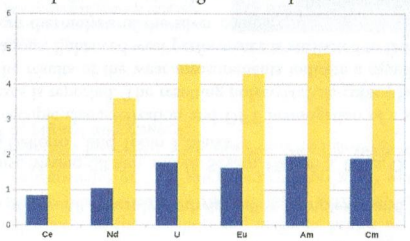

4698 dx.doi.org/10.1021/ic500388s

Ba_2HgS_5—A Molecular Trisulfide Salt with Dumbbell-like $(HgS_2)^{2-}$ Ions
Saiful M. Islam, Jino Im, Arthur J. Freeman, and Mercouri G. Kanatzidis*

Ba_2HgS_5 is a semiconducting polysulfide salt with a bandgap of 2.4 eV. Ba_2HgS_5 is a molecular salt consisting of linear complexes of $(HgS_2)^{2-}$, v-shaped S_3^{2-} ions, and interstitial Ba^{2+} cations. It is a semiconducting material with a bandgap of 2.4 eV. Crystal structure and Raman spectrum of Ba_2HgS_5.

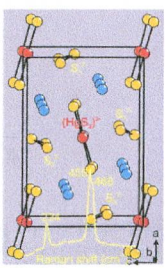

4705 S dx.doi.org/10.1021/ic500402m

Coinage Metal Complexes Supported by the Tri- and Tetraphosphine Ligands

Minh Thuy Dau, Julia R. Shakirova, Antti J. Karttunen, Elena V. Grachova,* Sergey P. Tunik,* Alexey S. Melnikov, Tapani A. Pakkanen, and Igor O. Koshevoy*

A family of tri- and tetranuclear complexes of Cu^{I}, Ag^{I}, and Au^{I} supported by the polydentate phosphines exhibit moderate to strong photoluminescence at room temperature in the solid state with quantum yields reaching 64%. Increase of the gold content within the cluster core gradually improves the quantum efficiency of these luminophores. The phosphorescence observed originates from the triplet excited states, determined by the metal cluster-centered $d_{\sigma^*} \rightarrow p_{\sigma}$ transitions.

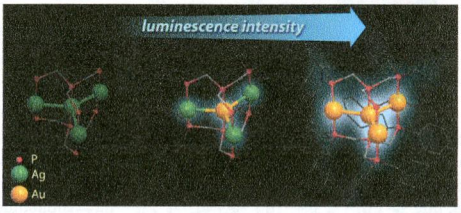

4716 S dx.doi.org/10.1021/ic500413j

Magnetic Sponge Phenomena Associated with Interchain Dipole–Dipole Interactions in a Series of Ferrimagnetic Chain Compounds Doped with Minor Diamagnetic Species

Masaki Nishio and Hitoshi Miyasaka*

A charge-transferred chain compound of the $[Ru_2]$/TCNQ series was isolated for the first time. The compound had a ferrimagnetic spin arrangement of $S = 3/2$ and $S = 1/2$ with $J/k_B \approx -100$ K and long-range antiferromagnetic ordering at $T_N \approx 11$ K. This material undergoes a crystal-to-crystal transition involving solvent elimination to give a new crystal phase with $T_N \approx 14$ K. Doping with $[Rh_2^{II,II}]$ modifies the T_N, the magnitude of the shift being dependent on the doping ratio, despite the fact that no significant structural changes were occurring.

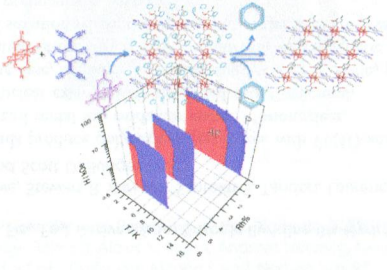

4724 S dx.doi.org/10.1021/ic500449d

Valence State Driven Site Preference in the Quaternary Compound $Ca_5MgAgGe_5$: An Electron-Deficient Phase with Optimized Bonding

Siméon Ponou,* Sven Lidin, Yuemei Zhang, and Gordon J. Miller*

The crystal structure of $Ca_5MgAgGe_5$ corresponds to the previously missing member of the structural series $R_{2+n}T_2X_{2+n}$, with $n = 3$. The orthorhombic space group *Pnma*, indicates a *klassengleiche* symmetry reduction of index two from the predicted space group *Cmcm*. It also represents a beautiful example of intermetallic phase where factors beyond the Zintl concept, such as the electrostatic valency principle and the chemical potential, are decisive for its stability and for the Mg/Ag site preference.

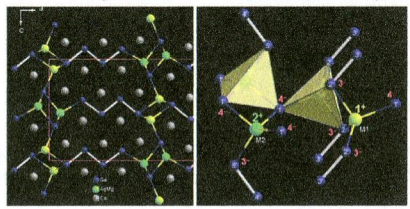

4733 S dx.doi.org/10.1021/ic5004885

Mixed-Ligand Approach to Design of Heterometallic Single-Source Precursors with Discrete Molecular Structure

Craig M. Lieberman, Anantharamulu Navulla, Haitao Zhang, Alexander S. Filatov, and Evgeny V. Dikarev*

A heterometallic single-source precursor with a discrete molecular structure was obtained via a mixed-ligand approach by using a combination of electron-withdrawing/electron-donating groups that allows changing the connectivity pattern within the heterometallic assembly.

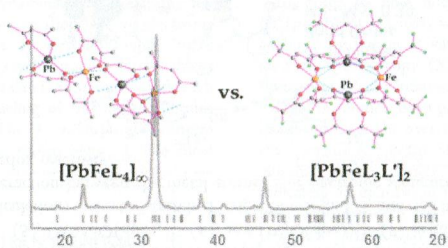

4739 S dx.doi.org/10.1021/ic500498k

Reactions of the Unsaturated Ditungsten Complexes $[W_2Cp_2(\mu\text{-}PPh_2)_2(CO)_x]$ (x = 1, 2) with Nitric Oxide: Stereoselective Carbonyl Displacement and Oxygen-Transfer Reactions of a Nitrite Ligand

M. Angeles Alvarez, M. Esther García, Daniel García-Vivó,* Sonia Melón, Miguel A. Ruiz,* and Adrián Toyos

The title complexes react with NO to give selectively either *cis*- or *trans*-dinitrosyl derivatives $[W_2Cp_2(\mu\text{-}PPh_2)_2(NO)_2]$ (Cp = η^5-C_5H_5), depending on the starting substrate, due to stereochemical inversion during reaction, involving η^2-C_5H_5 dinitrosyl intermediates. Trace amounts of oxygen promote formation of the nitrito complex $[W_2Cp_2(\mu\text{-}PPh_2)_2(ONO)(CO)(NO)]$, a thermally unstable species able to transfer oxygen to either the carbonyl or phosphido ligands, depending on reaction conditions.

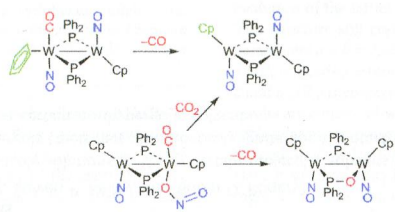

4751 dx.doi.org/10.1021/ic500526k

Synthesis, Redox Properties, and Electronic Coupling in the Diferrocene Aza-dipyrromethene and azaBODIPY Donor–Acceptor Dyad with Direct Ferrocene–α-Pyrrole Bond

Christopher J. Ziegler,* Kullapa Chanawanno, Abed Hasheminsasab, Yuriy V. Zatsikha, Eranda Maligaspe, and Victor N. Nemykin*

The novel diiron 3,3′-diferrocenylazapyrromethene (**3**) and its difluoroboron (azaBODIPY) derivative (**4**) were synthesized and characterized by UV–vis, NMR, electrochemistry, spectroelectrochemistry, and X-ray crystallographic methods, while their spectroscopy and redox behavior were correlated with the density functional theory (DFT) and time-dependent DFT calculations.

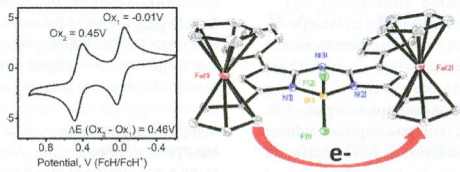

4756 dx.doi.org/10.1021/ic500548v

Variable Framework Structures and Centricities in Alkali Metal Yttrium Selenites, $AY(SeO_3)_2$ (A = Na, K, Rb, and Cs)

Seong-eun Bang, Dong Woo Lee, and Kang Min Ok*

A series of novel alkali metal yttrium selenites, $AY(SeO_3)_2$ (A = Na, K, Rb, and Cs), have been synthesized through hydrothermal reactions. The cation size and the coordination environment play important roles in determining the channel structures and space groups of the materials.

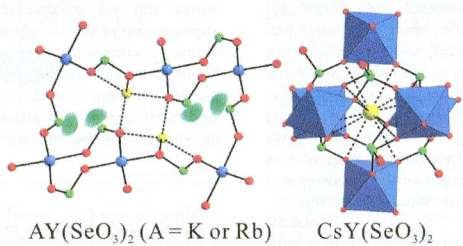

4763 dx.doi.org/10.1021/ic500594f

Cooperative Effect of Anion and Mole Ratio on the Coordination Modes of an NO_2S_3-Donor Macrocycle

Hyeong-Hwan Lee, In-Hyeok Park, and Shim Sung Lee*

The anion-controlled endo- and exocoordinated mercury(II) complexes with a macrocycle were isolated. Further, the mole ratio variation of the reactants undergoes the reaction resulting in an endo-/exocoordinated species.

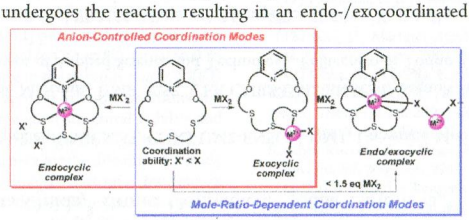

4770 Ⓢ dx.doi.org/10.1021/ic500622f

Nonaborane and Decaborane Cluster Anions Can Enhance the Ignition Delay in Hypergolic Ionic Liquids and Induce Hypergolicity in Molecular Solvents

Parker D. McCrary, Patrick S. Barber, Steven P. Kelley, and Robin D. Rogers*

$[B_{10}H_{13}]^-$ and $[B_9H_{14}]^-$ can form stable solutions in ILs or certain molecular solvents leading to enhanced ignition in known hypergols (fuels that spontaneously ignite upon contact with an oxidizer) or induced hypergolicity in certain nonhypergolic solvents.

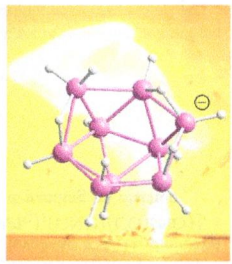

4777 Ⓢ dx.doi.org/10.1021/ic5007204

Oxidative Stretching of Metal–Metal Bonds to Their Limits

David W. Brogden, Yevgeniya Turov, Michael Nippe, Giovanni Li Manni, Elizabeth A. Hillard, Rodolphe Clérac, Laura Gagliardi, and John F. Berry*

The compounds $[Cr_2(dpa)_4]^{2+}$ (**1**), $[Mo_2(dpa)_4]^{2+}$ (**2**), $[MoW(dpa)_4]^{2+}$ (**3**), and $[W_2(dpa)_4]^{2+}$ (**4**) react with oxygen atom donors to yield $[Mo_2O(dpa)_4]^{2+}$ (**5**), $[WMoO(dpa)_4]^{2+}$ (**6**), and $[W_2O(dpa)_4]^{2+}$ (**7**) featuring a linear M···M≡O structure. DFT and CASSCF/CASPT2 calculations indicate "stretched" triple bonds in **2**, **3**, and **4**. The longer metal–metal distances in **5**, **6**, and **7** suggest minimal interaction between the metal atoms. The electronic structure of these complexes is used to rationalize their multielectron redox reactivity.

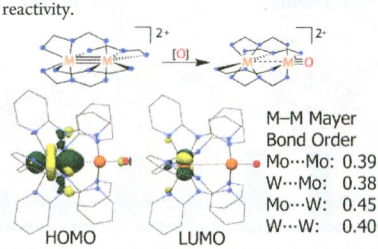

Ⓢ Supporting Information available via online article